

**Observation of the decay  $\Upsilon(4S) \rightarrow \Upsilon(1S)\pi^+\pi^-$** 

A. Sokolov,<sup>11</sup> M. Shapkin,<sup>11</sup> K. Abe,<sup>7</sup> K. Abe,<sup>41</sup> I. Adachi,<sup>7</sup> H. Aihara,<sup>43</sup> D. Anipko,<sup>1</sup> T. Aushev,<sup>12,17</sup> A. M. Bakich,<sup>38</sup> E. Barberio,<sup>20</sup> M. Barbero,<sup>6</sup> I. Bedny,<sup>1</sup> K. Belous,<sup>11</sup> U. Bitenc,<sup>13</sup> I. Bizjak,<sup>13</sup> A. Bondar,<sup>1</sup> M. Bračko,<sup>7,13,19</sup> T. E. Browder,<sup>6</sup> A. Chen,<sup>23</sup> W. T. Chen,<sup>23</sup> B. G. Cheon,<sup>3</sup> R. Chistov,<sup>12</sup> Y. Choi,<sup>37</sup> Y. K. Choi,<sup>37</sup> S. Cole,<sup>38</sup> J. Dalseno,<sup>20</sup> M. Dash,<sup>47</sup> A. Drutskoy,<sup>4</sup> S. Eidelman,<sup>1</sup> D. Epifanov,<sup>1</sup> S. Fratina,<sup>13</sup> T. Gershon,<sup>7</sup> A. Go,<sup>23</sup> G. Gokhroo,<sup>39</sup> B. Golob,<sup>13,18</sup> H. Ha,<sup>15</sup> J. Haba,<sup>7</sup> T. Hara,<sup>30</sup> Y. Hasegawa,<sup>36</sup> K. Hayasaka,<sup>21</sup> H. Hayashii,<sup>22</sup> M. Hazumi,<sup>7</sup> D. Heffernan,<sup>30</sup> Y. Hoshi,<sup>41</sup> S. Hou,<sup>23</sup> W.-S. Hou,<sup>24</sup> Y. B. Hsiung,<sup>24</sup> T. Iijima,<sup>21</sup> K. Inami,<sup>21</sup> A. Ishikawa,<sup>43</sup> R. Itoh,<sup>7</sup> M. Iwasaki,<sup>43</sup> Y. Iwasaki,<sup>7</sup> J. H. Kang,<sup>48</sup> P. Kapusta,<sup>25</sup> N. Katayama,<sup>7</sup> H. Kawai,<sup>2</sup> T. Kawasaki,<sup>27</sup> H. R. Khan,<sup>44</sup> H. Kichimi,<sup>7</sup> H. J. Kim,<sup>16</sup> Y. J. Kim,<sup>5</sup> S. Korpar,<sup>19,13</sup> P. Križan,<sup>13,18</sup> P. Krokovny,<sup>7</sup> R. Kulasiri,<sup>4</sup> R. Kumar,<sup>31</sup> A. Kuzmin,<sup>1</sup> Y.-J. Kwon,<sup>48</sup> T. Lesiak,<sup>25</sup> A. Limosani,<sup>7</sup> S.-W. Lin,<sup>24</sup> D. Liventsev,<sup>12</sup> F. Mandl,<sup>10</sup> T. Matsumoto,<sup>45</sup> S. McOnie,<sup>38</sup> W. Mitaroff,<sup>10</sup> H. Miyake,<sup>30</sup> H. Miyata,<sup>27</sup> Y. Miyazaki,<sup>21</sup> T. Nagamine,<sup>42</sup> Y. Nagasaka,<sup>8</sup> I. Nakamura,<sup>7</sup> E. Nakano,<sup>29</sup> M. Nakao,<sup>7</sup> Z. Natkaniec,<sup>25</sup> S. Nishida,<sup>7</sup> O. Nitoh,<sup>46</sup> T. Nozaki,<sup>7</sup> S. Ogawa,<sup>40</sup> T. Ohshima,<sup>21</sup> S. Okuno,<sup>14</sup> Y. Onuki,<sup>27</sup> H. Ozaki,<sup>7</sup> H. Palka,<sup>25</sup> C. W. Park,<sup>37</sup> H. Park,<sup>16</sup> L. S. Peak,<sup>38</sup> R. Pestotnik,<sup>13</sup> L. E. Piilonen,<sup>47</sup> Y. Sakai,<sup>7</sup> T. Schietinger,<sup>17</sup> O. Schneider,<sup>17</sup> C. Schwanda,<sup>10</sup> A. J. Schwartz,<sup>4</sup> R. Seidl,<sup>9,33</sup> M. E. Sevier,<sup>20</sup> H. Shibuya,<sup>40</sup> B. Shwartz,<sup>1</sup> A. Somov,<sup>4</sup> N. Soni,<sup>31</sup> S. Stanič,<sup>28</sup> H. Stoeck,<sup>38</sup> T. Sumiyoshi,<sup>45</sup> S. Suzuki,<sup>34</sup> F. Takasaki,<sup>7</sup> K. Tamai,<sup>7</sup> N. Tamura,<sup>27</sup> M. Tanaka,<sup>7</sup> G. N. Taylor,<sup>20</sup> Y. Teramoto,<sup>29</sup> X. C. Tian,<sup>32</sup> T. Tsukamoto,<sup>7</sup> S. Uehara,<sup>7</sup> T. Uglov,<sup>12</sup> S. Uno,<sup>7</sup> P. Urquijo,<sup>20</sup> Y. Usov,<sup>1</sup> G. Varner,<sup>6</sup> S. Villa,<sup>17</sup> C. C. Wang,<sup>24</sup> Y. Watanabe,<sup>44</sup> J. Wiechczynski,<sup>25</sup> E. Won,<sup>15</sup> C.-H. Wu,<sup>24</sup> B. D. Yabsley,<sup>38</sup> A. Yamaguchi,<sup>42</sup> Y. Yamashita,<sup>26</sup> M. Yamauchi,<sup>7</sup> L. M. Zhang,<sup>35</sup> Z. P. Zhang,<sup>35</sup> V. Zhilich,<sup>1</sup> and A. Zupanc<sup>13</sup>

(Belle Collaboration)

<sup>1</sup>*Budker Institute of Nuclear Physics, Novosibirsk*<sup>2</sup>*Chiba University, Chiba*<sup>3</sup>*Chonnam National University, Kwangju*<sup>4</sup>*University of Cincinnati, Cincinnati, Ohio 45221*<sup>5</sup>*The Graduate University for Advanced Studies, Hayama, Japan*<sup>6</sup>*University of Hawaii, Honolulu, Hawaii 96822*<sup>7</sup>*High Energy Accelerator Research Organization (KEK), Tsukuba*<sup>8</sup>*Hiroshima Institute of Technology, Hiroshima*<sup>9</sup>*University of Illinois at Urbana-Champaign, Urbana, Illinois 61801*<sup>10</sup>*Institute of High Energy Physics, Vienna*<sup>11</sup>*Institute of High Energy Physics, Protvino*<sup>12</sup>*Institute for Theoretical and Experimental Physics, Moscow*<sup>13</sup>*J. Stefan Institute, Ljubljana*<sup>14</sup>*Kanagawa University, Yokohama*<sup>15</sup>*Korea University, Seoul*<sup>16</sup>*Kyungpook National University, Taegu*<sup>17</sup>*Swiss Federal Institute of Technology of Lausanne, EPFL, Lausanne*<sup>18</sup>*University of Ljubljana, Ljubljana*<sup>19</sup>*University of Maribor, Maribor*<sup>20</sup>*University of Melbourne, Victoria*<sup>21</sup>*Nagoya University, Nagoya*<sup>22</sup>*Nara Women's University, Nara*<sup>23</sup>*National Central University, Chung-li*<sup>24</sup>*Department of Physics, National Taiwan University, Taipei*<sup>25</sup>*H. Niewodniczanski Institute of Nuclear Physics, Krakow*<sup>26</sup>*Nippon Dental University, Niigata*<sup>27</sup>*Niigata University, Niigata*<sup>28</sup>*University of Nova Gorica, Nova Gorica*<sup>29</sup>*Osaka City University, Osaka*<sup>30</sup>*Osaka University, Osaka*<sup>31</sup>*Panjab University, Chandigarh*<sup>32</sup>*Peking University, Beijing*<sup>33</sup>*RIKEN BNL Research Center, Upton, New York 11973*<sup>34</sup>*Saga University, Saga*<sup>35</sup>*University of Science and Technology of China, Hefei*

<sup>36</sup>*Shinshu University, Nagano*<sup>37</sup>*Sungkyunkwan University, Suwon*<sup>38</sup>*University of Sydney, Sydney NSW*<sup>39</sup>*Tata Institute of Fundamental Research, Bombay*<sup>40</sup>*Toho University, Funabashi*<sup>41</sup>*Tohoku Gakuin University, Tagajo*<sup>42</sup>*Tohoku University, Sendai*<sup>43</sup>*Department of Physics, University of Tokyo, Tokyo*<sup>44</sup>*Tokyo Institute of Technology, Tokyo*<sup>45</sup>*Tokyo Metropolitan University, Tokyo*<sup>46</sup>*Tokyo University of Agriculture and Technology, Tokyo*<sup>47</sup>*Virginia Polytechnic Institute and State University, Blacksburg, Virginia 24061*<sup>48</sup>*Yonsei University, Seoul*

(Received 15 November 2006; published 17 April 2007)

We study transitions between  $Y$  states with the emission of charged pions using  $477 \text{ fb}^{-1}$  of data collected with the Belle detector at the KEKB asymmetric-energy  $e^+e^-$  collider. The measured product branching fraction  $\mathcal{B}(Y(4S) \rightarrow Y(1S)\pi^+\pi^-) \times \mathcal{B}(Y(1S) \rightarrow \mu^+\mu^-) = (4.42 \pm 0.81(\text{stat}) \pm 0.56(\text{sys})) \times 10^{-6}$ . When the PDG value for  $\mathcal{B}(Y(1S) \rightarrow \mu^+\mu^-)$  is used, this corresponds to  $\mathcal{B}(Y(4S) \rightarrow Y(1S)\pi^+\pi^-) = (1.78 \pm 0.33(\text{stat}) \pm 0.23(\text{sys})) \times 10^{-4}$  and a partial decay width  $\Gamma(Y(4S) \rightarrow Y(1S)\pi^+\pi^-) = (3.65 \pm 0.67(\text{stat}) \pm 0.65(\text{sys})) \text{ keV}$ .

DOI: [10.1103/PhysRevD.75.071103](https://doi.org/10.1103/PhysRevD.75.071103)

PACS numbers: 13.25.Gv

The bottomonium state  $Y(4S)$  has a mass above the threshold for  $B\bar{B}$  pair production and decays mainly into  $B$ -meson pairs ( $\mathcal{B}(Y(4S) \rightarrow B\bar{B}) > 96\%$  [1]). However, the decay modes  $Y(4S) \rightarrow Y(mS)\pi\pi$  with  $m = 1, 2$  should exist. The *BABAR* Collaboration has published the first observation of dipion decays to both  $Y(1S)$  and  $Y(2S)$  [2]; Ref. [3] presented preliminary evidence for the decay  $Y(4S) \rightarrow Y(1S)\pi^+\pi^-$ . A similar decay mode of the charmonium state  $\psi(3770)$  has been observed [4]. In this paper we report the observation of the decay mode  $Y(4S) \rightarrow Y(1S)\pi^+\pi^-$  from the Belle experiment. This measurement supersedes our preliminary results [3,5].

We use  $477 \text{ fb}^{-1}$  of data collected on the  $Y(4S)$  resonance and in the nearby continuum to study  $Y(4S) \rightarrow Y(1S)\pi^+\pi^-$  decays with a subsequent  $Y(1S) \rightarrow \mu^+\mu^-$  transition. Charged particles are reconstructed and identified in the Belle detector [6], which consists of a central drift chamber (CDC), aerogel threshold Cherenkov counters (ACC), time-of-flight (TOF) scintillation counters, an electromagnetic calorimeter (ECL), and a  $K_L$ -muon detector (KLM). We require that charged tracks be well-measured and consistent with originating from the interaction point. Charged particles are assigned a likelihood  $\mathcal{L}_i$  [7] ( $i = \mu, \pi, K$ ) based on the matching of hits in the KLM to the track extrapolated from the CDC, and identified as muons if the likelihood ratio  $P_\mu = \mathcal{L}_\mu / (\mathcal{L}_\mu + \mathcal{L}_\pi + \mathcal{L}_K) > 0.8$ , corresponding to a muon detection efficiency of approximately 91.5% over the polar angle range  $20^\circ \leq \theta \leq 155^\circ$  and the momentum range  $0.7 \text{ GeV}/c \leq p \leq 3.0 \text{ GeV}/c$  in the laboratory frame. Electron identification uses a similar likelihood ratio  $P_e$  [8] based on CDC, ACC, and ECL information. Charged particles that are not identified as muons and have a likelihood ratio  $P_e < 0.05$  are treated as pions.

Identification of  $\gamma$ s is based on information from the ECL. Calorimeter clusters not associated with reconstructed charged tracks and with energies greater than 50 MeV are considered as  $\gamma$  candidates.

Candidates for  $Y(4S) \rightarrow Y(1S)\pi^+\pi^-$  decays with the subsequent leptonic decay  $Y(1S) \rightarrow \mu^+\mu^-$  are selected from the standard Belle hadronic event sample. The most important selection criteria for this event sample are the following: multiplicity of charged tracks in an event  $N_{\text{ch}} \geq 3$ ; the event's visible energy  $E_{\text{vis}} \geq 0.2\sqrt{s}$ , where  $\sqrt{s}$  is the center-of-mass (c.m.) energy; the sum of good cluster energies in the ECL must satisfy  $0.1 \leq E_{\text{sum}}/\sqrt{s} \leq 0.8$ ; the sum of the  $z$  components of each charged track's and photon's momenta is required to satisfy  $|P_z| < 0.5\sqrt{s}$ . The variables  $E_{\text{vis}}$ ,  $E_{\text{sum}}$ ,  $P_z$  are evaluated in the c.m. system.

To select  $Y(1S) \rightarrow \mu^+\mu^-$  decays, hadronic events are required to contain a  $\mu^+\mu^-$  pair with  $M_{\mu^+\mu^-} > 9 \text{ GeV}/c^2$  and also to satisfy  $10.5 \text{ GeV} < E_{\text{vis}}^{\text{lab}} < 12.5 \text{ GeV}$ , where  $E_{\text{vis}}^{\text{lab}}$  is the event's visible energy calculated in the laboratory frame. The latter requirement reduces background from poorly reconstructed events. After these requirements,  $1.32 \times 10^5$  events remain. We then require the presence of a  $\pi^+\pi^-$  pair. To reduce background from  $Y(1S)$  production in radiative return processes [9] with the subsequent conversion of the emitted photon into an  $e^+e^-$  pair that is misidentified as  $\pi^+\pi^-$ , we impose an additional requirement on the angle between the pion momenta in the laboratory system:  $\cos\theta_{\pi\pi} < 0.95$ . The number of selected events is 1084.

To observe resonance states that decay into the  $Y(1S)\pi^+\pi^-$  final state, the distribution of the mass difference  $\Delta M = (M_{\mu^+\mu^-\pi^+\pi^-} - M_{\mu^+\mu^-})$  with  $M_{\mu^+\mu^-}$  in the range  $|M_{\mu^+\mu^-} - m_{Y(1S)}| < 60 \text{ MeV}/c^2$  is examined (see

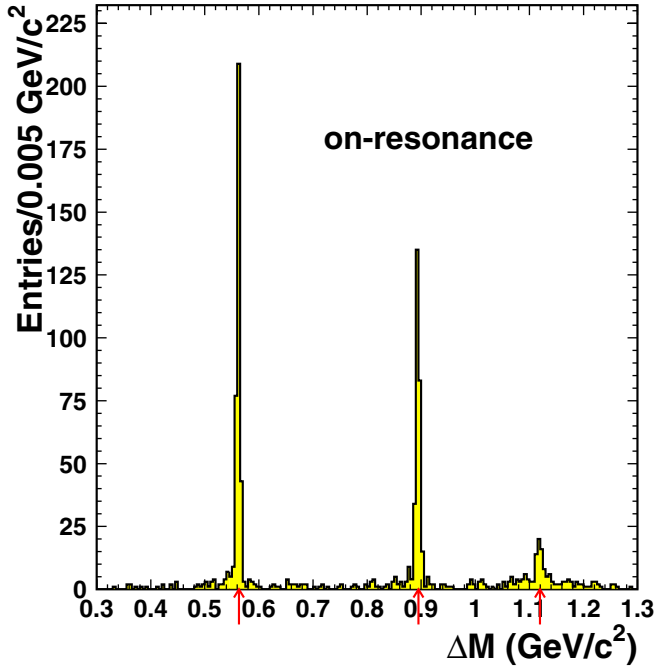


FIG. 1 (color online). The mass difference  $\Delta M = (M_{\mu^+\mu^-\pi^+\pi^-} - M_{\mu^+\mu^-})$  distribution where  $M_{\mu^+\mu^-}$  lies in the  $\Upsilon(1S)$  mass region. Arrows show the positions of the mass differences  $(m_{\Upsilon(2S)} - m_{\Upsilon(1S)})$ ,  $(m_{\Upsilon(3S)} - m_{\Upsilon(1S)})$ , and  $(m_{\Upsilon(4S)} - m_{\Upsilon(1S)})$ , respectively, based on PDG values.

Fig. 1) for the on-resonance sample. Here  $m_{\Upsilon(1S)}$  is the nominal  $\Upsilon(1S)$  mass.

Three peaks are seen in the  $\Delta M$  distribution. The first, second, and third peaks are at  $\sim 560$ ,  $890$ , and  $1120$   $\text{MeV}/c^2$ , respectively. The first and second peaks have very little background. Fits to the first two peaks using Gaussians for the signal shapes result in peak positions of  $(561.7 \pm 0.1)$   $\text{MeV}/c^2$  and  $(893.4 \pm 0.2)$   $\text{MeV}/c^2$ . These values are compatible with the  $(m_{\Upsilon(2S)} - m_{\Upsilon(1S)})$  and  $(m_{\Upsilon(3S)} - m_{\Upsilon(1S)})$  PDG [1] values, respectively. We conclude that the first and second peaks are due to the decays  $\Upsilon(2S) \rightarrow \Upsilon(1S)\pi^+\pi^-$  and  $\Upsilon(3S) \rightarrow \Upsilon(1S)\pi^+\pi^-$ , where the  $\Upsilon(2S, 3S)$  are produced mainly in the radiative return processes  $e^+e^- \rightarrow \Upsilon(2S, 3S)\gamma$ .

In contrast to the first two peaks, the third peak has modest background. The position of the peak is derived from a fit to the  $\Delta M$  distribution in the third peak region (see Fig. 2) using a Gaussian for the signal and a third order polynomial for the background. The result is  $\Delta M = (1119.2 \pm 0.4)$   $\text{MeV}/c^2$ , which is in good agreement with the mass difference  $(m_{\Upsilon(4S)} - m_{\Upsilon(1S)})$  from the PDG. The Gaussian width is  $\sigma = (5.7 \pm 1.0)$   $\text{MeV}/c^2$ , which is consistent with the estimated  $\Delta M$  resolution. The signal yield in the interval  $1110$   $\text{MeV}/c^2 < \Delta M < 1135$   $\text{MeV}/c^2$  determined from the fit is  $N_{\text{ev}} = 43.9 \pm 7.9$ , with a statistical significance of  $8.0\sigma$  which corresponds to  $-2 \ln(\mathcal{L}_0/\mathcal{L}_{\text{max}}) = 72.3$  with 3 degrees of freedom (mass, width, and yield). Here  $\mathcal{L}_0$  and  $\mathcal{L}_{\text{max}}$  are

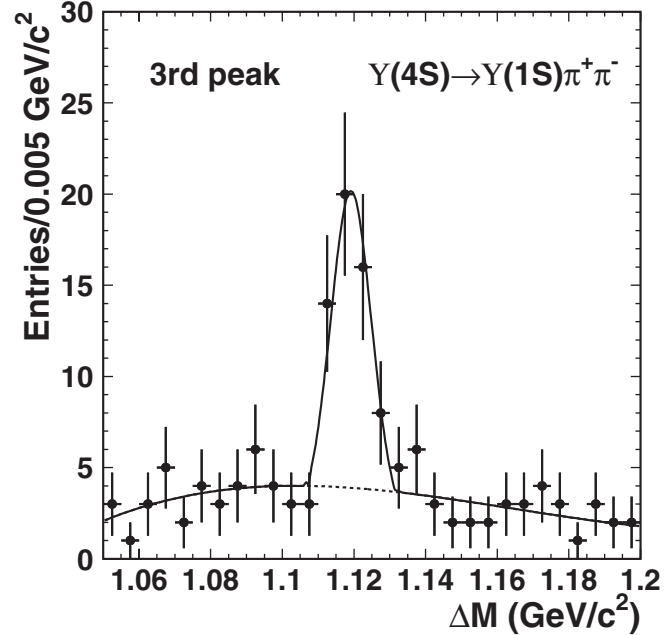


FIG. 2. The fit to the third peak in the  $\Delta M$  distribution ( $|M_{\mu^+\mu^-} - m_{\Upsilon(1S)}| < 60$   $\text{MeV}/c^2$ ) using a Gaussian for the signal and a third order polynomial for the background (dotted line). The solid line shows the sum of a Gaussian and a polynomial function.

the likelihood values returned by the fit with signal yield fixed at zero and its best fit value, respectively. This peak is identified as a signal for the decay  $\Upsilon(4S) \rightarrow \Upsilon(1S)\pi^+\pi^-$  with a subsequent  $\Upsilon(1S) \rightarrow \mu^+\mu^-$  transition.

To verify this interpretation, we study the resonance properties in more detail. First, the  $\Delta M$  distribution for the  $(\mu^+\mu^-\pi^+\pi^-X)$  event sample in the  $M_{\mu^+\mu^-} > 8$   $\text{GeV}/c^2$  mass region is considered. Here we use a looser requirement on  $M_{\mu^+\mu^-}$  to study the background in a wider region. The distribution of  $\Delta M$  vs  $M_{\mu^+\mu^-}$  for the on-resonance (off-resonance,  $\sqrt{s} = 10.52$   $\text{GeV}$ , integrated luminosity  $\int \mathcal{L} dt = 49.4$   $\text{fb}^{-1}$ ) sample is shown in Fig. 3(a), 3(b).

Comparing the two distributions, we see that the behavior for the on-resonance and off-resonance sample are similar except that in the off-resonance data, the third peak is absent. The “slanted band” in this plot is due to the nonresonant reaction  $e^+e^- \rightarrow \mu^+\mu^-\pi^+\pi^-$ .

Using the off-resonance sample, the  $\Delta M$  distribution where  $M_{\mu^+\mu^-}$  is restricted to  $|M_{\mu^+\mu^-} - m_{\Upsilon(1S)}| < 60$   $\text{MeV}/c^2$  has only two peaks, corresponding to  $\Upsilon(2S)$  and  $\Upsilon(3S)$  decays. For the on-resonance sample when the data size is scaled to the off-resonance sample, the total number of events and the number of background events in the interval  $1110$   $\text{MeV}/c^2 < \Delta M < 1135$   $\text{MeV}/c^2$  is  $N_{\text{tot}}^{\text{res}} = (7.3 \pm 0.9)$  and  $N_{\text{bkg}}^{\text{res}} = (2.2 \pm 0.5)$ , respectively. If we consider a  $\Delta M$  interval shifted by  $-60$   $\text{MeV}/c^2$ , to take the lower  $\sqrt{s}$  into account, we find  $N_{\text{tot}}^{\text{off}} = (3.0 \pm 1.7)$

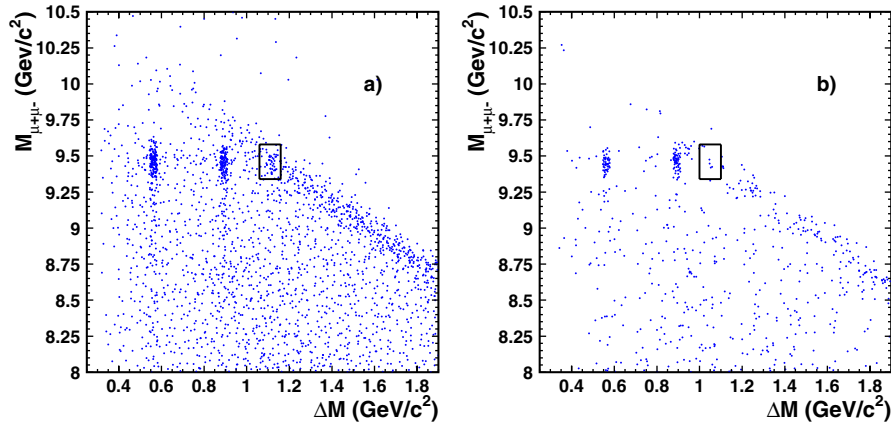


FIG. 3 (color online). The  $\Delta M$  vs  $M_{\mu^+\mu^-}$  scatter plot for the on-resonance sample (a) and off-resonance sample (b) in the  $M_{\mu^+\mu^-} > 8$   $\text{GeV}/c^2$  mass region. The rectangle in (a) indicates where  $Y(4S) \rightarrow Y(1S)\pi^+\pi^-$  transitions would cluster; the  $q\bar{q}$  background in this region should scale from that in the rectangle in (b). For clarity, the rectangle in (a) is drawn larger than the region used to determine the signal yield (which is determined by optimizing the expected signal yield relative to the square root of the expected background).

events in the off-resonance sample. To compare the scaled total ( $N_{\text{tot}}^{\text{res}}$ ) and background ( $N_{\text{bkg}}^{\text{res}}$ ) yields as models for the off-resonant yield  $N_{\text{tot}}^{\text{off}}$ , we use the so-called likelihood  $\chi^2$  [10]. We find  $\chi^2 = 0.26$  for  $N_{\text{bkg}}^{\text{res}}$ , and  $\chi^2 = 3.26$  for  $N_{\text{tot}}^{\text{res}}$ : the background interpretation of the events in the third peak region is therefore favored, although the discrimination is relatively weak ( $1.7\sigma$ ). This suggests that the events in the third peak region show no sign of a similar enhancement.

The “slanted band” in Fig. 3 is well described by the background from the process  $e^+e^- \rightarrow \mu^+\mu^-\pi^+\pi^-$ . The modelling of this process with phase space confirms this. The distribution of events, which are located in this band over the variable  $z = (M_{\mu^+\mu^-} - 0.982 \cdot \Delta M)$  which gives the change along the “slanted band” have a clear peak at  $z = (8347.9 \pm 8.7)$   $\text{MeV}/c^2$  in the on-resonance sample and no peak in the off-resonance one near this range. This peak corresponds to the decay  $Y(4S) \rightarrow Y(1S)\pi^+\pi^-$ . The background under the peak estimated from the fit and from sidebands is  $N_{\text{bkg}}^{\text{fit}} = 73.6$  and  $N_{\text{bkg}}^{\text{sb}} = (74 \pm 7.9)$ , respectively. After scaling to the off-resonance sample the background is  $N_{\text{bkg}}^{\text{scale}} = (8.6 \pm 0.9)$ , which is compatible with the number of events in the off-resonance sample in the same range  $N_{\text{bkg}}^{\text{off}} = (9 \pm 3)$ . Thus, we have a good agreement between all methods of background estimation.

Additional information can be obtained from the study of the  $\pi^+\pi^-$  system. The efficiency-corrected distribution of the invariant mass of the  $\pi^+\pi^-$  system ( $M_{\pi^+\pi^-}$ ) is shown in Fig. 4 for events in the third peak region. The background (see Fig. 2) is not subtracted from the  $M_{\pi^+\pi^-}$  distribution. The efficiency is calculated by a Monte Carlo simulation. The EvtGen event generator [11] with a matrix element [12] taking into account particle spins is used to produce  $Y(4S) \rightarrow Y(1S)\pi^+\pi^- \rightarrow \mu^+\mu^-\pi^+\pi^-$  events

that are passed through the detector simulation and reconstruction programs.

As shown in Fig. 4, the  $M_{\pi^+\pi^-}$  distribution for events from the third peak region in the  $\Delta M$  distribution shows an enhancement at high masses. In contrast, the distribution for background events, which is taken from the  $\Delta M$  sideband ( $1004$   $\text{MeV}/c^2 < \Delta M < 1110$   $\text{MeV}/c^2$ ,  $1135$   $\text{MeV}/c^2 < \Delta M < 1210$   $\text{MeV}/c^2$ ) and normalized

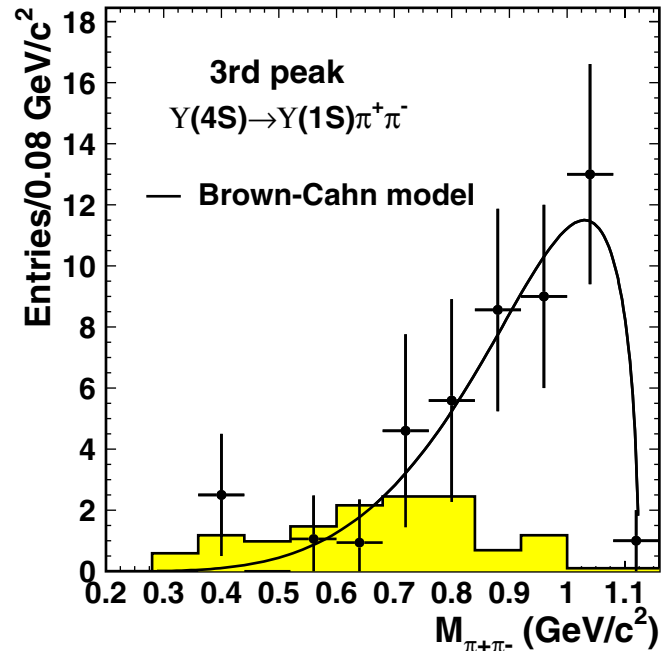


FIG. 4 (color online). The  $\pi^+\pi^-$  invariant mass distributions for events from the third peak region in the  $\Delta M$  distribution. The shaded histogram is for background events estimated from the  $\Delta M$  sideband. The solid line shows the  $\Delta M$  distribution predicted by the Brown-Cahn model [12].

to the background events underneath the peak, is more uniform and shows no sign of a similar enhancement. This difference in the behavior of the  $M_{\pi^+\pi^-}$  distribution is an additional argument in favor of a resonance interpretation of the third peak.

The  $M_{\pi^+\pi^-}$  distribution can be described by the shape predicted by the Brown-Cahn model [12] (see Fig. 4), where the hadronic transition between heavy quarkonia is considered as a two-step process: the emission of gluons from heavy quarks and subsequent conversion of these gluons into light hadrons.

The branching fraction for the  $Y(4S) \rightarrow Y(1S)\pi^+\pi^-$  decay is determined from  $\mathcal{B}(Y(4S) \rightarrow Y(1S)\pi^+\pi^-) = N_{\text{ev}}/(N_{Y(4S)} \cdot \varepsilon \cdot \mathcal{B}(Y(1S) \rightarrow \mu^+\mu^-))$ . The total number of  $Y(4S)$  in the data sample is  $N_{Y(4S)} = (464 \pm 6) \times 10^6$ , and the nominal branching fraction  $\mathcal{B}(Y(1S) \rightarrow \mu^+\mu^-) = (2.48 \pm 0.05)\%$  [1]. The efficiency obtained from the Monte Carlo sample is  $\varepsilon = (2.14 \pm 0.06)\%$ . We apply a correction of about 8% to  $E_{\text{sum}}/\sqrt{s}$ , one of the variables used for selecting hadronic events. The efficiency is sensitive to this variable; the correction is designed so that the data and MC match in this variable.

The systematic error in the reconstruction efficiency due to this correction is 8%. The systematic uncertainty in the reconstruction efficiency due to lack of knowledge of the  $Y(4S) \rightarrow Y(1S)\pi^+\pi^- \rightarrow \mu^+\mu^-\pi^+\pi^-$  decay matrix element is estimated by varying the parameterization of the  $M_{\pi^+\pi^-}$  distribution. Requiring a reasonable fit to the  $M_{\pi^+\pi^-}$  distribution (we allow a  $\chi^2$  change of  $\pm 1\sigma$ ) we find a 3% variation in the efficiency. We fit the background in the sideband region using a third order polynomial. The systematic uncertainty from changing the sideband range ( $1035 \div 1055 \text{ MeV}/c^2$ ,  $1210 \div 1250 \text{ MeV}/c^2$ ) and from varying the order of the background polynomial from three to two is 4.5%. Other systematic uncertainties come from the choice of the signal range (4%), choice of the  $Y(1S)$  mass range (6%), and from the tracking efficiency (4%). The total systematic uncertainty is obtained by adding these contributions in quadrature; the result is 13%.

The measured product branching fraction is

$$\begin{aligned} \mathcal{B}(Y(4S) \rightarrow Y(1S)\pi^+\pi^-) \times \mathcal{B}(Y(1S) \rightarrow \mu^+\mu^-) \\ = (4.42 \pm 0.81(\text{stat}) \pm 0.56(\text{sys})) \times 10^{-6}. \end{aligned}$$

The branching fraction is

$$\begin{aligned} \mathcal{B}(Y(4S) \rightarrow Y(1S)\pi^+\pi^-) \\ = (1.78 \pm 0.33(\text{stat}) \pm 0.23(\text{sys})) \times 10^{-4}. \end{aligned}$$

We also extract the partial decay width for  $Y(4S) \rightarrow Y(1S)\pi^+\pi^-$  transition using the world-average value of the total width [1] and obtain

$$\begin{aligned} \Gamma(Y(4S) \rightarrow Y(1S)\pi^+\pi^-) \\ = (3.65 \pm 0.67(\text{stat}) \pm 0.65(\text{sys})) \text{ keV}. \end{aligned}$$

The product branching fraction from *BABAR* [2] is  $= (2.23 \pm 0.25(\text{stat}) \pm 0.27(\text{sys})) \times 10^{-6}$ , which differs by 2.1 standard deviations from the presented here.

To summarize, a study of transitions between  $Y$  states with the emission of charged pions has been performed at Belle. The mass difference distribution ( $M_{\mu^+\mu^-\pi^+\pi^-} - M_{\mu^+\mu^-}$ ) from the  $\mu^+\mu^-\pi^+\pi^-X$  event sample for  $M_{\mu^+\mu^-}$  within the  $Y(1S)$  mass region has two peaks from  $Y(2S, 3S) \rightarrow Y(1S)\pi^+\pi^-$  decays with no background. A third peak at  $\Delta M = (1119.2 \pm 0.4) \text{ MeV}/c^2$  is interpreted as a signal for the decay  $Y(4S) \rightarrow Y(1S)\pi^+\pi^-$  with a subsequent  $Y(1S) \rightarrow \mu^+\mu^-$  transition. This final state is the first example of a non- $B\bar{B}$  decay mode of the  $Y(4S)$ . The branching fraction  $\mathcal{B}(Y(4S) \rightarrow Y(1S)\pi^+\pi^-)$  and the partial decay width  $\Gamma(Y(4S) \rightarrow Y(1S)\pi^+\pi^-)$  are measured. The  $M_{\pi^+\pi^-}$  distribution can be described by the shape predicted by the Brown-Cahn model [12].

We thank the KEKB group for excellent operation of the accelerator, the KEK cryogenics group for efficient solenoid operations, the KEK computer group, and the NII for valuable computing and Super-SINET network support. We acknowledge support from MEXT and JSPS (Japan); ARC and DEST (Australia); NSFC and KIP of CAS (contract No. 10575109 and IHEP-U-503, China); DST (India); the BK21 program of MOEHRD, and the CHEP SRC and BR (grant No. R01-2005-000-10089-0) programs of KOSEF (Korea); KBN (contract No. 2P03B 01324, Poland); MIST (Russia); ARRS (Slovenia); SNSF (Switzerland); NSC and MOE.

- [1] W.-M. Yao *et al.* (Particle Data Group), *J. Phys. G* **33**, 1 (2006).  
 [2] B. Aubert *et al.* (*BABAR* Collaboration), *Phys. Rev. Lett.* **96**, 232001 (2006).  
 [3] K. Abe *et al.* (Belle Collaboration), hep-ex/0512034.  
 [4] J. Z. Bai *et al.* (BES Collaboration), *Phys. Lett. B* **605**, 63

- (2005); N. E. Adam *et al.* (CLEO Collaboration), *Phys. Rev. Lett.* **96**, 082004 (2006).  
 [5] The large change in the branching fraction  $\mathcal{B}(Y(4S) \rightarrow Y(1S)\pi^+\pi^-)$  is due to a significant improvement in the efficiency calibration.  
 [6] A. Abashian *et al.* (Belle Collaboration), *Nucl. Inst. and*

A. SOKOLOV *et al.*

Meth. A **479**, 117 (2002).

- [7] A. Abashian *et al.* (Belle Collaboration), Nucl. Inst. and Meth. A **491**, 69 (2002).
- [8] K. Hanagaki *et al.*, Nucl. Inst. and Meth. A **485**, 490 (2002).
- [9] M. Benayoun *et al.*, Mod. Phys. Lett. A **14**, 2605 (1999).

PHYSICAL REVIEW D **75**, 071103(R) (2007)

- [10] S. Baker and R. Cousins, Nucl. Inst. and Meth. **221**, 437 (1984).
- [11] D.J. Lange, Nucl. Inst. and Meth. A **462**, 152 (2001).
- [12] L. S. Brown and R. N. Cahn, Phys. Rev. Lett. **35**, 1 (1975); M. B. Voloshin, JETP Lett. **21**, 347 (1975); T.-M. Yan, Phys. Rev. D **22**, 1652 (1980).